The use of Grating Lock-in IR thermography for the determination of thermal properties

G.Kalogiannakis*, H.Zhang, C.Glorieux
Laboratory of Acoustics and Thermal Physics, Katholieke Universiteit Leuven, Belgium

J.Ravi
Centre for Excellence in Lasers and Optoelectronic Science (CELOS), Cochin University of Science and Technology, India

S.Longuemart
Laboratory of Thermophysics of Condensed Matter (group of UMR CNRS 8024), University of Littoral Cote d'Opale, France

D. Van Hemelrijck
Dept. Mechanics of Materials and Constructions, Vrije Universiteit Brussel, Belgium

*Georgios.Kalogiannakis@fys.kuleuven.be

Abstract - In this study, we demonstrate the use of grating lock-in IR thermography for the determination of the thermal conductivity of composite materials. This technique is based on the use of a spatially modulated heating pattern. The latter results in the formation of a similarly modulated temperature field and the thermal properties are determined via their influence to the modulation depth. In lock-in thermography, the excitation source is also temporally modulated at a certain frequency which results in a higher signal-to-noise ratio. This method leads to the simplification of the ill-posed problem of the thermal properties' determination. Moreover, the right placement of the grating allows separating the influence of the conductivities in each direction in order to obtain better accuracy.

Keywords: thermography, grating, thermal characterization, composite materials.

1 Introduction

In the last decade, a lot of progress has been achieved both in the theoretical description as well as the experimental implementation regarding the thermal characterization of anisotropic solids and composite materials in particular. Significant research [1-11] has been dedicated to model thermal wave scattering from various subsurface structures including planar inclusions, spheres and cylinders. This research group has also used the mirage method to successfully characterize the anisotropy of unidirectional fiber reinforced composites. Similar results were experimentally obtained by Lauriks et al. [12] for carbon fiber reinforced composites.

Krapez et al. [13] recently presented a variation of the flash method where a pulsed heat source was combined with a grid-like mask for the determination of the thermal diffusivity of inhomogeneous media. Wu et al. [14] and Karpen et al. [15-16] have carried out experiments on composites using harmonic waves. The same group has developed a semi-analytical model [16], which uses a recursive algorithm [17] to find the solution in the Fourier coordinates. Then, an inverse FFT transforms the temperature to the Cartesian spatial coordinates allowing a fast numerical simulation of the thermal wave field at the surface of multilayered composites assumed to have an infinite absorption coefficient. The latter assumption limits the investigation on carbon fiber reinforced composites, as, from the typically used fibers, carbon only has a very high absorption coefficient at the laser wavelength. Still, it has been proven in practice that, because of the rather transparent epoxy matrix, the absorption coefficient can not be considered infinite for carbon composites either.

Our model is based on an analytical solution adapted for a multilayer system that allows different finite absorption coefficients for each layer [18]. Thus, on one hand it is fast and on the other hand it is more accurate. Moreover, it can accommodate composite materials with fibers other than carbon like glass or kevlar and mixtures of them in different layers and it can be used to find the temperature distribution in planes other than the surface, providing, if required, a 3D view of the field. Finally, this theory can be easily adapted for different source geometries.

In what follows, there is first a short overview of the theory related to grating IR thermography describing the

formation of the temperature field at the surface and how it can be used for the determination of the thermal properties. In the second part, this theory is applied for the determination of the properties of a unidirectional Carbon/Epoxy composite material.

2 Grating IR thermography

2.1 Theoretical model

Our analytical solution for multilayer composites is based on the so-called transfer function formalism [19]. A laser induced heat source is amplitude modulated at a certain frequency and is combined with a square wave filtering pattern to generate a laterally modulated thermal wave field in space.

The starting point of the analysis is the heat diffusion equation for a single ply of a composite material. A single ply is an orthotropic material, which has by definition, at least two orthogonal planes of symmetry, where material properties are independent of direction. In such a material, thermal conductivity is not scalar but a tensor. In the principal axes coordinate system (which coincide with the axes parallel and perpendicular to the fibers), the heat diffusion equation for a single ply is expressed as follows:

$$k_{\parallel}\frac{\partial^2 T_s}{\partial x^2}+k_{\perp}\frac{\partial^2 T_s}{\partial y^2}+k_{\perp}\frac{\partial^2 T_s}{\partial z^2}-\rho C\frac{\partial T_S}{\partial t}=Q \tag{1}$$

where $k_{||}$(W/mK) and $k_{\perp}$(W/mK) are the thermal conductivities parallel and vertically to the fibers, ρ (kg/m^3) is the density, C (J/kgK) is the specific heat of the material, Q (W/m^3) is the periodically modulated heat source intensity given by,

$$Q=\frac{I_0}{2}\beta e^{-\beta z}e^{i\omega t}g(x,y) \tag{2}$$

where I_0 (W/m^2) is the optical intensity, β (m^{-1}) is the optical absorption coefficient, ω (rad/sec) is the excitation frequency and $g(x,y)$ is dimensionless and quantifies the shape of the excitation in the x-y plane.

The shape of the source that describes the grating distribution $g(x,y)$ is:

$$g(x,y)=\frac{1}{2}e^{-\left(\frac{x^2}{R_X{}^2}+\frac{y^2}{R_Y{}^2}\right)}\left\{1+\mathrm{sgn}\left[\sin\left(\frac{2\pi(x-x_0)}{\lambda}\right)\right]\right\} \tag{3}$$

where R_X and R_Y are the dimensions of the beam in the x- and y- direction respectively in the case of cylindrical focusing, x_0 is the position of the grating with respect to the origin of the coordinate system and λ is the wavelength of the grating.

If the orthogonal coordinate system xyz is rotated with an angle θ from the principal directions, the expression of the heat diffusion in a single ply is changed as follows:

$$k_{xx}\frac{\partial^2 T}{\partial x^2}+k_{yy}\frac{\partial^2 T}{\partial y^2}+k_{zz}\frac{\partial^2 T}{\partial z^2}+\left(k_{xy}+k_{yx}\right)\frac{\partial^2 T}{\partial x\partial y}=$$
$$=\rho C\frac{\partial T}{\partial t}+Q \tag{4}$$

with

$$k_{xx}=k_{\parallel}\cos^2\theta+k_{\perp}\sin^2\theta,\quad k_{yy}=k_{\perp}\cos^2\theta+k_{\parallel}\sin^2\theta$$
$$k_{xy}=k_{yx}=\left(k_{\perp}-k_{\parallel}\right)\sin\theta\cos\theta,\quad k_{zz}=k_{\perp} \tag{5}$$

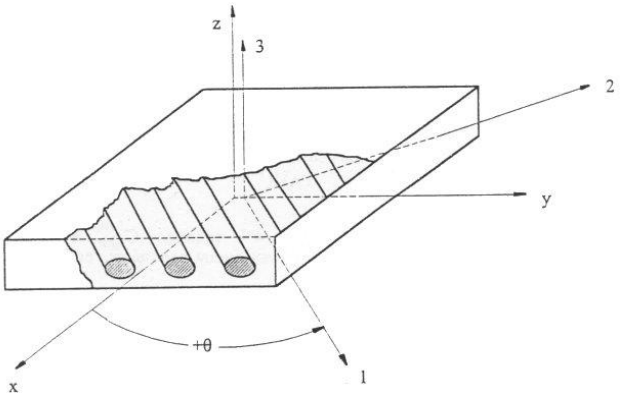

Figure 1: Rotation from the natural (global) to the principal coordinate system.

Assuming a harmonic time dependence of the solution, after applying a Fourier transform in the time domain and a 2-D Fourier transform in the spatial domain (xy-plane), the diffusion equation reduces to an ordinary second order differential equation with respect to the third spatial coordinate:

$$a\frac{\partial^2\tilde{T}}{\partial z^2}+b\frac{\partial\tilde{T}}{\partial z}+c\tilde{T}=\frac{I_0}{2}\beta e^{-\beta z}\tilde{G}\left(f_x,f_y\right) \tag{6}$$

where:

$$\tilde{T}\left(f_x, f_y, z\right) = \int\int_{-\infty}^{+\infty} T\left(x, y, z\right) e^{-2j\pi\left(f_x x + f_y y\right)} dxdy \quad (7)$$

$$\tilde{G}\left(f_x, f_y\right) = \int\int_{-\infty}^{+\infty} g\left(x, y\right) e^{-2j\pi\left(f_x x + f_y y\right)} dxdy \quad (8)$$

$$\begin{aligned} a &= k_{zz} \\ b &= 0 \\ c &= -4\pi^2\left[k_{xx} f_x^2 + k_{yy} f_y^2 + 2k_{xy} f_x f_y\right] - j\omega\rho C \end{aligned} \quad (9)$$

and f_x, f_y are the Fourier coordinates. The coefficients a, b and c have a different influence on the formation of the temperature field. While a is mainly related to the transfer of energy along z, b describes beam steering effects and, in the case of multilayered composites, it equals zero. c indicates a preferential spreading of the spectrum, depending on the various conductivities, which result in the loss of the field symmetry.

The general solution of eq.(6) consists of the solution of the homogeneous equation and the particular solution for the considered excitation. For a single layer, it can be written as:

$$\tilde{T}\left(f_x, f_y, z, \omega\right) = U\left(f_x, f_y, \omega\right) e^{m_1 z} + V\left(f_x, f_y, \omega\right) e^{m_2 z} + \\ + F\left(f_x, f_y, z, \omega\right) \quad (10)$$

where

$$F\left(f_x, f_y, z, \omega\right) = \frac{1}{2}\left(\frac{1}{a\beta^2 + c}\right) I_0 \beta e^{-\beta z} \tilde{G}\left(f_x, f_y\right) \quad (11)$$

and,

$$m_{1,2} = \pm\sqrt{\frac{4\pi^2\left[k_{xx} f_x^2 + k_{yy} f_y^2 + 2k_{xy} f_x f_y\right] + j\omega\rho C}{k_{zz}}} \quad (12)$$

where U, V (K) are coefficients which are to be found from the boundary conditions related to temperature and heat flux continuity and $m_{1,2}$ (m^{-1}) is the effective complex thermal wavenumber along the z–axis. The real part of the inverse quantity $1/m_{1,2}$ represents the effective thermal diffusion length along the z–axis.

Since composite materials consist of a stack of thin layers, when a localized external heat source is applied, the thermal-wave field is formed according to the contribution of the different layers. The anisotropy of each of the layers within the reach of thermal diffusion in the time scale of the modulation adds a unique feature to the thermal response at the surface.

Each layer (lamina) composing the laminate is unidirectional, elastically and thermally orthotropic, with its thermal conductivity given in global coordinates by eq.(5). Every layer i is characterized by the thermal conductivity coefficient tensor k_i and the scalar density ρ_i, the specific heat c_i, the absorption coefficient β_i and the thickness l_i. It is assumed in our study that there is no reflection of light at the interfaces between layers and that all properties are constant within a layer. The harmonic power density in the i-th layer is given by the Beer-Lambert law expressed as follows:

$$Q_i = \frac{I_0 . \beta_i . g\left(x, y\right)}{2} \exp\left[-\bar{\beta}_{i-1} + \beta_i\left(z + \bar{l}_{i-1}\right)\right] \exp\left(j\omega t\right) \quad (13)$$

where

$$\bar{\beta}_{i-1} = \sum_{n=1}^{i-1} \beta_n l_n \quad \text{and} \quad \bar{l}_{i-1} = \sum_{n=1}^{i-1} l_n$$

The layers of the composite lie perpendicular to the z-axis and the boundaries of the laminate are in contact with infinitely extended air. The equations can be solved in a straightforward way for a multilayered geometry to provide the thermal wave field at any depth considering the continuity of temperatures and heat flows at the interfaces. This continuity is equivalently valid in the temporally and spatially Fourier-transformed solution, just as in the Cartesian formulation. Considering N layers, applying these boundary conditions yields a set of 2N linear equations of the 2N unknown coefficients:

$$\mathbf{A} \cdot \mathbf{U} = \mathbf{F} \quad (14)$$

which can be solved very fast for a reasonable number of layers. In eq.(14), A is a matrix that depends on the thermal properties, experimental and geometric characteristics, U is the vector of the unknown coefficients and F is the vector describing the applied forces in each layer. A detailed description about setting up the equations to be solved can be found in [18]. The three-dimensional Fourier-transformed temperature field can thus be determined for every value of f_x,f_y,z and **W** .

To find the time harmonic solution in the Cartesian coordinates, one has to apply the inverse Fourier transform:

$$T\left(x, y, z, \omega\right) = \int\int_{-\infty}^{+\infty} \tilde{T}\left(f_x, f_y, z, \omega\right) e^{2j\pi\left(f_x x + f_y y\right)} df_x df_y \quad (15)$$

The most convenient way to evaluate eq.(15), is by applying fast Fourier transform (FFT) [16], which is

much faster than numerical integration [13]. Karpen et al. [16] discuss some possible problems with FFT, but provided a laterally wide enough integration range and sufficiently fine discretization, we do not encounter any problems.

2.2 Properties' determination process

The inverse problem, which is to extract the thermal properties from the experimentally assessed thermal wave field, is ill-posed and complicated. Moreover, the inverse problem is numerically very demanding in terms of computing time, because a number of iterations are needed to converge from an initial guess to the actual solution. This initial guess is therefore also crucial in the process.

The optothermal properties of a composite material are the thermal conductivities parallel and perpendicular to the fibers, or k_1, k_2 and k_3 (in the case that the lateral thermal conductivity perpendicular to the fibers is not equal to the one across the thickness), the specific heat C, and the absorption coefficient β. The simplest configuration to determine these properties is to perform experiments on a simple, thermally thick (theoretically semi-infinite) unidirectional laminate. The 3D thermal-wave problem is then reduced into solving a simple 2x2 set of equations. The surface solution in the Fourier space is then given by:

$$\Theta_0\left(f_x, f_y, \omega\right) = \frac{I_0}{2}\left(\frac{\beta}{\beta + m_1}\right)\left(\frac{1}{k_a m_0 + k_\perp m_1}\right)\tilde{G}\left(f_x, f_y\right) \tag{16}$$

where β (m^{-1}) is the absorption coefficient of the composite and m_0, m_1 (m^{-1}) are the effective thermal wave numbers in the air and the semi-infinite composite respectively given by:

$$m_0 = \sqrt{4\pi^2\left(f_x + f_y\right)^2 + \frac{j\omega}{\alpha_a}} \tag{17}$$

with $\alpha_a = \dfrac{k_a}{\rho_a C_a}$ (m^2/s)

being the thermal diffusivity of air, and

$$m_1 = \sqrt{\frac{4\pi^2\left[k_\parallel f_x^2 + k_\perp f_y^2\right] + j\omega\rho C}{k_\perp}} \tag{18}$$

To solve this problem in practice, we have to define an area large enough to describe the thermal-wave field (the temperature amplitude at the edges of the area must be negligible) and avoid thus aliasing. Then the area is discretized densely enough to find convergence to the desired level of accuracy.

The analytical solution in the simple case when uniform illumination is combined with a grating, which is a sinusoidal spatial filter is shown to be given by:

$$\Theta_G\left(f_x, \omega\right) = \frac{I_0}{2}\left(\frac{\beta}{\beta + m_1}\right)\left(\frac{1}{k_a m_0 + k_\perp m_1}\right) \cdot \left\{\frac{j}{2}\left[\delta\left(f_x + \frac{1}{\lambda}\right) - \delta\left(f_x - \frac{1}{\lambda}\right)\right]\right\} \tag{19}$$

where δ is the Dirac function and m_0, m_1 (m^{-1}) are given in this case by:

$$m_0 = \sqrt{4\pi^2 f_x^{\,2} + \frac{j\omega}{\alpha_a}} \tag{20}$$

and

$$m_1 = \sqrt{\frac{4k_\parallel \pi^2 f_x^2 + j\omega\rho C}{k_\perp}} \quad \text{or} \quad \sqrt{\frac{4k_\perp \pi^2 f_x^2 + j\omega\rho C}{k_\perp}} \tag{21}$$

depending whether the filter is positioned vertically or parallel to the fibers respectively. The inverse Fourier transform of eq.(19) gives the resulting temperature oscillation in space. The modulation depth of the temperature amplitude and phase can be easily determined from the absolute difference of the extremes of the modulation.

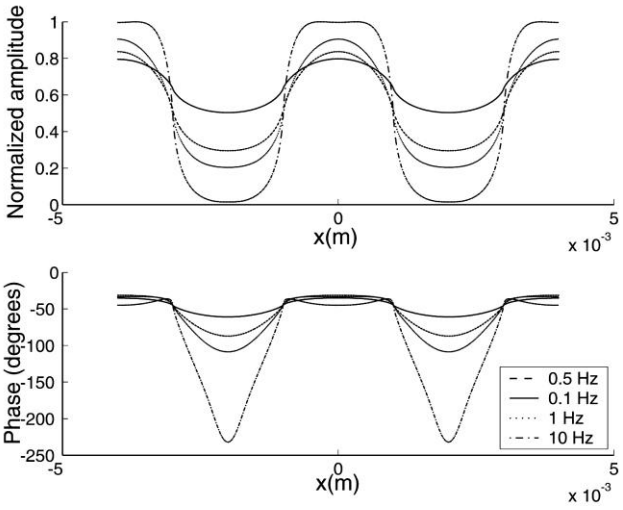

Figure 2: Normalized amplitude and phase modulation of temperature perpendicularly to the grating bands (λ=4mm) and the fibers as a function of frequency. The material is semi-infinite unidirectional composite with $k_{\perp}$=1W/mK, C=800J/kgC and ρ=1550kg/m^3 in contact with air.

A typical view of the resulting photothermal field is depicted in Figure 2 for a composite material with with $k_{\perp}$=1W/mK, C=800J/kgC and ρ=1550kg/m^3 in contact with air.

The measurement is no more bound to the excitation geometry of conventional approaches (radius or line width of the source) and the previously fitted field is reduced to fitting two values, the amplitude of the field's normalized amplitude and phase modulation with respect to excitation frequency. The only *a priori* condition is that the excitation frequency has to be low enough so that the thermal waves from the opposite sides of an unheated zone due to the grating have effective wavelengths of the order of $\lambda/4$ so as to interfere with one another. As can be seen in Figure 2 the modulation amplitude is naturally reduced with lower frequency as a result of longer thermal diffusion length and increased washing out of periodical warm and cold zones.

In order to evaluate the properties one has to perform a series of measurements for different grating spacings and a logarithmically scaled frequency range. Then the curves of the modulated amplitude and phase can be either fitted for a fixed frequency and the entire set of gratings or for a fixed grating and the whole frequency range. Even more appropriately, one has to fit the most sensitive region of the frequency range for multiple gratings. As the sensitive part of the excitation frequency range depends on the grating spacing, one has to move to larger spacings for lower frequencies and vice versa (Fig.3). The material properties used for the simulation shown in this example are:

$$k_{\perp} = 0.56\ \text{W/mK},\ C = 793\ \text{J/KgK},\ \rho = 1550\ \text{Kg/m}^3 \quad (22)$$

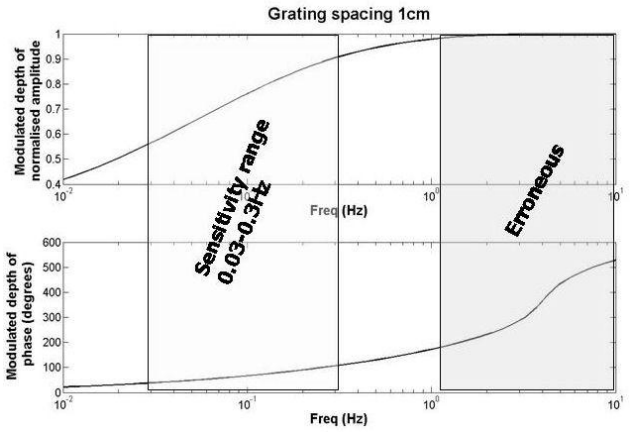

Figure 3: The sensitive part of the excitation frequency range depends on the grating spacing.

3 Experiments

Preliminary experiments were performed on a 5mm thick unidirectional carbon/epoxy material $[0°]_{40}$ (provided by Hexcel– Fibredux 920CX-TS-5-42) with the experimental setup depicted in Figure 4. A diode laser beam (FAP I-Coherent Inc) is expanded and then goes through a square wave filter to apply a spatially modulated heating pattern. The temperature field is probed by means of an IR camera from CEDIP. A home-made lock-in application was developed in Labview using a DAQ card from National Instruments (NI-DAQ PCI5024E) to drive the laser and perform the lock-in procedure.

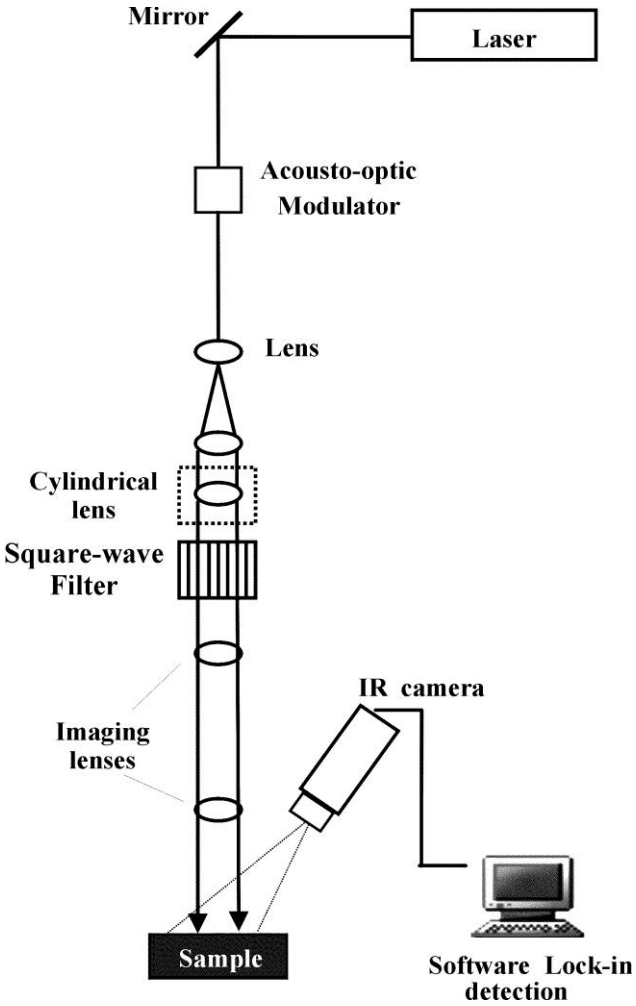

Figure 4: Experimental setup of grating IR thermography.

The noise sources that are encountered are either temporal or spatial and they must be both reduced in order to improve the accuracy and the reproducibility of a measurement. To reduce the temporal noise, we have to remove the background temperature fluctuations and realize a significant number of experiments so as to perform statistical analysis. On the other hand, to reduce the spatial noise one has to take into account the non-uniformity of the DC background, to deconvolve the gaussian or arbitrary shape of the heat source and integrate a few lines along the transverse direction (perpendicularly to the grating lines). A typical view of the field as it is measured by our system is shown in Figure 5 in terms of phase variation.

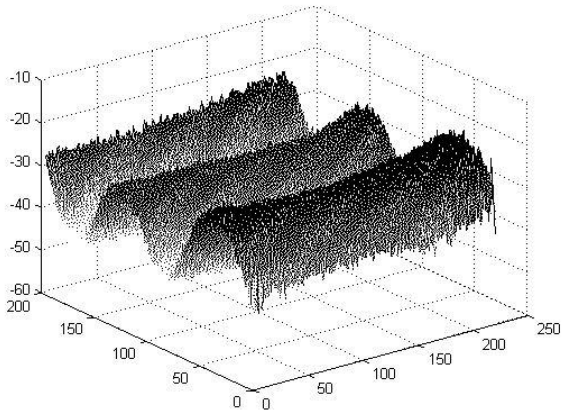

Figure 5: Phase variation at the surface of carbon/epoxy excited at 0.02Hz.

4 Results – Discussion

A series of measurements was carried out with a grating of 4mm wavelength. In what follows we show some preliminary results in order to demonstrate how the technique can be exploited in order to evaluate the thermal properties. The full potential is described elsewhere [18,20].

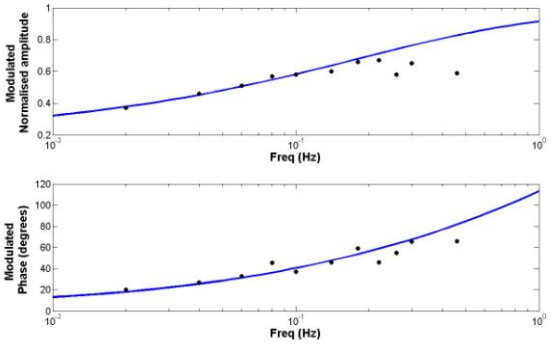

Figure 6: Manual fitting of the experimental data with the theoretical curves of the modulated temperature amplitude and phase for a carbon/epoxy laminate and a grating of 4mm.

In this preliminary test, we have considered the carbon/epoxy described in the previous section, which has been also tested earlier [21] with Modulated Temperature Differential Scanning Calorimetry (MTDSC) [22]. With the latter technique, we determined the thermal conductivity perpendicular to the fibers and the specific heat (eq.22). Then, having placed the grating perpendicular to the fibers, grating IR thermography was used to fit manually the modulated amplitude and phase

in order to determine the thermal conductivity along the fibers. The result is shown in Fig.6. Since only three measurements were taken and taking into account that the noise is typically reduced in lower frequencies it is natural that the curve is not well fitted at the high frequency end. However, at low frequencies the fit is very good even for this low number of measurements and demonstrates the potential of the method. The thermal conductivity along the fibers was estimated around 3W/mK but more elaborated results with more gratings and actual fitting will be found in [20].

5 Conclusions

A novel technique has been developed to determine the thermal properties of materials. The fact that it allows selection of a direction of interest makes it particularly suitable for composite materials, where thermal conductivity and thermal diffusivity are not scalar but tensors.

References

[1] A.Ocariz, A.Sanchez-Lavega and A.Salazar. Journal de Physique – Colloques, 4(7): 583-586, 1994
[2] A.Ocariz, A.Sanchez-Lavega and A.Salazar. Appl. Phys. 81(11): 7552-7560, 1997.
[3] A.Ocariz, A.Sanchez-Lavega and A.Salazar. Appl. Phys. 81(11): 7561-7566, 1997.
[4] A.Salazar, A.Sanchez-Lavega, A.Ocáriz, J.Guitonny, J.C.Pandey, D.Fournier and A.C.Boccara. Appl. Phys.Lett., 67(5): 626-628, 1995.
[5] A.Salazar, A.Sanchez-Lavega, A.Ocáriz, J.Guitonny, J.C.Pandey, D.Fournier and A.C.Boccara. Appl.Phys. 79(81): 3984-3993, 1996.
[6] A.Salazar, A.Sanchez-Lavega and A.Ocariz. Optical Engineering - Bellingham. 36(2): 391-399, 1997.
[7] A.Salazar and A.Sanchez-Lavega. Int.Jour.Therm. 19(2): 625, 1998.
[8] A.Salazar, J.M.Terron, A.Sanchez-Lavega and R.Cellorio. Appl.Phys.Lett. 80(11): 1903-1905, 2002.
[9] A.Salazar, A.Sanchez-Lavega and R.Cellorio. Appl.Phys. 93(8): 4536-4542, 2003.
[10] J.M.Terron, A.Salazar and A.Sanchez-Lavega. Appl.Phys. 89(10): 5696-5702, 2001.
[11] J.M.Terron, A.Salazar and A.Sanchez-Lavega. Appl. Phys. 91(3): 1087-1098, 2002.
[12] W.Lauriks, C.Desmet, C.Glorieux and J.Thoen. J.Mat.Res. 8(12): 3106-3110, 1993.
[13] J.C.Krapez, L.Spagnolo, M.Friess, H.S.Maier and G.Neuer. Int. J. Therm. Sci. 43(10): 967-978, 2004.
[14] D.Wu, R.Steegmuller, W.Karpen and G.Busse. In D.O. Thompson and D. E. Chimenti (editors), *Review of Progress in Quantitative nondestructive evaluation*, Plenum Press, New York, 14: 439-446, 1995.
[15] W.Karpen, D.Wu, R.Steegmuller and G.Busse. In D.Balageas, G.Busse and G.M.Carlomagno (editors), *Quantitative infrared thermography*, *Proc. QIRT '94. Paris*: Editions Européennes Thermique et Industrie , p. 281-286, 1995.
[16] W.Karpen, D.Wu and G.Busse. Res. Nondestr. Eval. 11: 179-197, 1999.
[17] P.Grosse and R.Wynands. Appl.Phys. 48:59, 1987.
[18] G.Kalogiannakis, S.Longuemart, J.Ravi, A.Okasha, D.Van Hemelrijck & C.Glorieux. J. Appl. Phys. 100 (6) , 2006.
[19] M.Vaez Iravani and M.Nikoonahad. Appl.Phys. 62(10): 4065-4071, 1987.
[20] G. Kalogiannakis, J.Ravi, H.Zhang, S.Longuemart, D.Van Hemelrijck & C.Glorieux, (in preparation to be submitted in *J. Appl. Phys.*)
[21] G.Kalogiannakis, D.Van Hemelrijck & G.Van Assche. J. of Comp. Mater., 38(2): 163-175, 2004.
[22] E1952-98 Standard method for thermal conductivity and thermal diffusivity by Modulated Temperature Differential Scanning Calorimetry (MTDSC). Annual Book of ASTM standards, 1998.